Modeling Approaches and Software for Predicting the Performance of Milling Operations at MAL- UBC

Y. Altintas, Professor
CIRP Member, ASME Fellow
University of British Columbia (UBC)
Manufacturing Automation Laboratory (MAL), http://www.mech.ubc.ca/~mal

ABSTRACT

The author has been conducting research in the area of metal cutting mechanics, metal cutting dynamics, machine tool vibrations, precision machining and machine tool control in his Manufacturing Automation Laboratory, at The University of British Columbia, Canada since 1986. This article summarizes the research conducted in mechanics and dynamics of metal cutting in our laboratory. Modeling of mechanics of metal cutting is summarized first. The models include orthogonal to oblique cutting transformation, mechanistic modeling of cutting coefficients, slip line field and Finite Element modeling. The author mostly focused on milling. The kinematics of milling with and without structural vibrations is modeled. The geometric model of end mills and inserted cutters with arbitrary geometry are modeled. The prediction of forces, torque, power and dimensional surface finish is explained for milling operations. The chatter stability for milling operations is presented. The metal cutting knowledge is transferred to manufacturing industry by combining all the models in shop friendly software.

1 INTRODUCTION

The purpose of this article is to review the research done at the author's laboratory, therefore the general review of the vast metal cutting literature is not covered in the article. The readers are referred to the recent review presented in CIRP by van Luttervelt et al. [1] and in ASME by Ehman et al. [2]

The metal cutting research should lead to improved design of cutting tools, machine tool structures, spindle and feed drives and the optimal planning of individual machining operations based on physical constraints. The amplitude and frequency of cutting forces, torque and power are used in sizing machine tool structures, spindle and feed drive mechanisms, bearings, motors and drives as well as the shank size of the tools and fixture rigidity. The stress and temperature field in the cutting tool edge, chip and finish work piece surface are used in designing cutting edge shape as well as in optimizing feed, speed and depth of cut to avoid residual stresses on the finish surface. Modeling the interaction between the cutting process and structural vibrations of machine tool, cutting tool and fixture leads to the identification of weak links in the machine structure and determination of chatter vibration free spindle speeds and depth of cuts [3]. The complete model of the machining process is therefore used in both design of cutting tools and machine tools, as well as planning of machining operations for maximum productivity and quality.

The article summarizes the models developed and adopted in the author's laboratory. The modeling of metal cutting mechanics is presented in section 2. The kinematics and mechanics of milling are presented in section 3, followed by chatter stability prediction in section 4. Several simulation and experimental results are presented for complex end mills and inserted cutters in section 5. The article is concluded with the current issues in machining research and technology transfer in section 6.

2 MECHANICS OF CUTTING

The first step is to model the cutting process as a function of work material, tool geometry and material, chip load and cutting speed. The macro-mechanics of cutting lead to the identification of cutting coefficients, which are used in predicting the cutting forces, torque, power and chatter stability limits. The cutting coefficients can be modeled using either orthogonal cutting mechanics or mechanistic models. The micro mechanics of metal cutting is on the other hand, is used to predict the stress, strain and temperature distribution in the chip and tool. It is primarily used for tool design, the analysis of material behavior under high strain and temperature, and optimal selection of chip load and speed to avoid tool chipping, tool wear, and residual stresses left on the finish surface.

2.1 Macro - Mechanics of Metal Cutting

The diagram of orthogonal cutting, where the plastic deformation is assumed to take place at a thin shear plane, is shown in Figure 1. The process is modeled by conducting orthogonal cutting tests, typically turning tubes with a wall thickness equal to the radial depth of cut (a). The orthogonal tool must have a sharp cutting edge with zero side cutting edge and inclination angles. The cutting force in the radial direction is zero in orthogonal cutting. The cutting forces in the tangential (F_t) and feed (F_f) directions are measured with a dynamometer, and chips are collected during each test. The measured forces are separated into shear (F_{tc},F_{fc})

and flank contact/ploughing (F_{te},F_{fe}) edge components as:

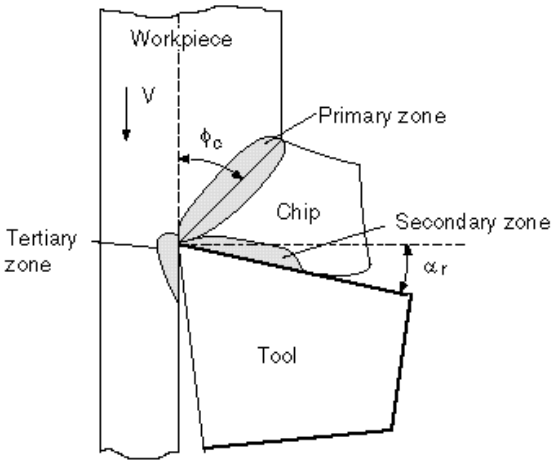

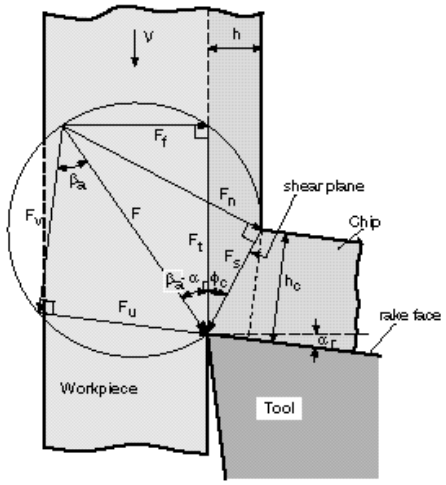

Cutting force diagram

Figure 1: Mechanics of orthogonal cutting process.

$$F_t = F_{tc} + F_{te} = K_{tc} ah + K_{te} a$$
$$F_f = F_{fc} + F_{fe} = K_{fc} ah + K_{fe} a \qquad (1)$$

The cutting forces are assumed to be linearly proportional to uncut chip area (h), and edge forces can be identified by extrapolating the measured forces at zero cut thickness (h = 0) intercept. The slopes of the linear force plots correspond to the cutting force coefficients (K_{tc},K_{fc}) in the tangential and feed directions. The thickness of the collected chips is measured and an average value is considered. The chip thickness (h_c) is more accurately predicted by measuring its length and weight. The specific weight and width of the chip are known, thus the chip thickness can be evaluated. The shear angle (f_c) of the primary deformation zone can be evaluated as:

$$r_c = \frac{h}{h_c}, \qquad \phi_c = \tan^{-1} \frac{r_c \cos \alpha_r}{1 - r_c \cos \alpha_r} \qquad (2)$$

where (r_c, α_r) are the chip compression ratio and rake angle of the orthogonal tool, respectively. The shear force (F_s) and average shear stress (t_s) on the primary deformation zone can be evaluated as:

$$F_s = F_{tc} \cos f_c - F_{fc} \sin f_c, \qquad \tau_s = \frac{F_s}{(ah / \sin \phi_c)} \qquad (3)$$

Depending on the lubrication, cutting speed and material type, the chip may first stick than slide on the rake face. In macro-mechanics, and average Coulomb friction angle (β_a) and friction coefficient (μ_a) are considered, and evaluated from the cutting force measurements as:

$$b_a = a_r + \arctan \frac{F_{fc}}{F_{tc}}, \qquad m_a = \tan b_a \qquad (4)$$

The resultant cutting force (F_c) can be expressed as a function of shear force as:

$$F_c = \frac{F_s}{\cos(f_c + b_a - a_r)} = \frac{t_s ah}{\sin f_c \cos(f_c + b_a - a_r)} \qquad (5)$$

The tangential and feed forces can be expressed as a function of resultant cutting force, which leads to the following:

$$F_{tc} = F_c \cos(b_a - a_r) = ah[t_s \frac{\cos(b_a - a_r)}{\sin f_c \cos(f_c + b_a - a_r)}]$$
$$F_{fc} = F_c \sin(b_a - a_r) = ah[t_s \frac{\sin(b_a - a_r)}{\sin f_c \cos(f_c + b_a - a_r)}] \qquad (6)$$

From equations (5),(6) the cutting coefficients can be expressed directly as a function of average shear stress, shear angle, average friction angle and rake angle of the tool :

$$K_{tc}\left[N/mm^2\right] = t_s \frac{\cos(b_a - a_r)}{\sin f_c \cos(f_c + b_a - a_r)}$$
$$K_{fc}\left[N/mm^2\right] = t_s \frac{\sin(b_a - a_r)}{\sin f_c \cos(f_c + b_a - a_r)} \qquad (7)$$

Once the cutting coefficients are identified, cutting forces for any depth of cut (*a*) and cut thickness (*h*) can be evaluated in an orthogonal cutting operation. When the cutting coefficients are found from the slope or trend of the force measurements, the method is called *mechanistic modeling*. When the cutting force coefficients are evaluated from the shear stress, shear angle and friction angle, the method is based on the *macro-mechanics of orthogonal cutting*. The mechanics approach relates the basic material property, friction and tool geometry directly to the magnitudes of cutting forces. Depending on the material behavior during machining, the three orthogonal cutting parameters (τ_s,ϕ_c,μ_a) may vary with the cut thickness (*h*), cutting speed (*V)* and rake angle (α_r). In order to cover wide range of cutting conditions, the orthogonal cutting tests must be conducted at a range of cutting speeds, feeds and rake angles. The orthogonal parameters can be curve fitted to empirical expressions to cover the range of cutting conditions used in experiments.

Mechanistic approach has been popular in predicting the cutting forces, torque and power very quickly for a set of tool geometry and work material. In early 1950s, Kienzle reported specific cutting coefficient tables, which were calibrated from extensive machining tests conducted on most common alloys by using different rake angles speeds, feeds [4]. Metcut also prepared an extensive Machining Data Handbook which contains cutting

coefficients and machinability conditions for commonly used alloys [5].

Most practical tools used in industry have oblique geometry, where the tools may have side cutting edge angle, nose radius or helix angle. There are cutting forces in all three directions, which have to be evaluated (Figure 2). In mechanistic approach, the slopes or trend of the measured cutting forces in all three directions are evaluated as in orthogonal cutting, see Eq. (5). Hence, each tool with a specific geometry must be calibrated in machining tests in order to find the cutting coefficients in mechanistic modeling. However, using macro-metal cutting mechanics approach, or *unified approach* as Armarego calls it [6], the cutting coefficients for any oblique tool can be predicted as follows:

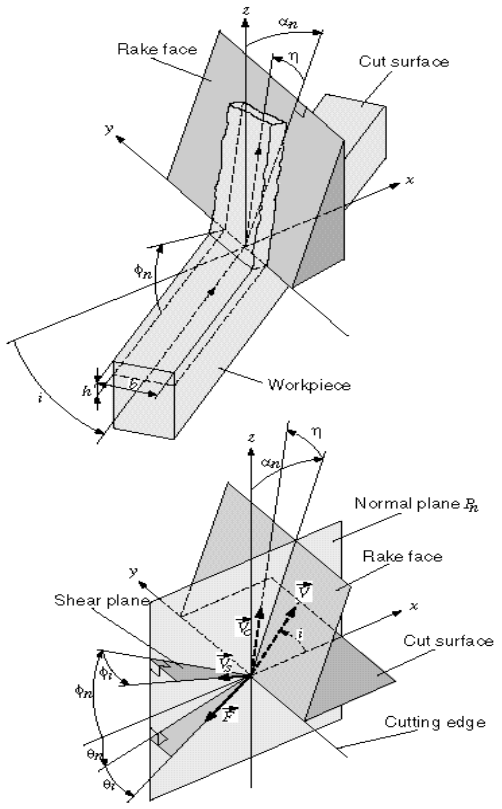

Figure 2: Mechanics of oblique cutting process.

$$K_{tc} = \frac{t_s}{\sin f_n} \frac{\cos(b_n - a_n) + \tan i \tan h \sin b_n}{\sqrt{\cos^2(f_n + b_n - a_n) + \tan^2 h \sin^2 b_n}}$$

$$K_{fc} = \frac{t_s}{\sin f_n \cos i} \frac{\sin(b_n - a_n)}{\sqrt{\cos^2(f_n + b_n - a_n) + \tan^2 h \sin^2 b_n}} \qquad (8)$$

$$K_{ac} = \frac{t_s}{\sin f_n} \frac{\cos(b_n - a_n)\tan i - \tan h \sin b_n}{\sqrt{\cos^2(f_n + b_n - a_n) + \tan^2 h \sin^2 b_n}}$$

where K_{ac} is the axial cutting coefficient for the force perpendicular to the cutting speed and uncut chip plane. Stabler assumed that the chip flow angle (η) is approximately equal to oblique angle (*i*), which can be used for practical force calculations, but not for tool design. The combined influence of rake and inclination angles must be considered for more accurate prediction of chip flow direction that is important for the evacuation of chip [1]. The normal shear angle (ϕ_n), friction angle (β_n) and shear stress (τ_s) in oblique cutting can be assumed to be identical to the values obtained from the orthogonal cutting tests described above. The normal rake angle of the oblique tool must be evaluated from the various angles of the oblique tool [6],[7].

2.2 Micro-Mechanics of Metal Cutting

The prediction of stress, strain, strain rate and temperature fields in the chip and tool wedge are important for tool and process design. The author's research group studied two techniques: Slip Line Field analysis technique as proposed by Oxley [8], and numerical techniques such as Finite Element and Finite Difference methods. The objective is to analyze the primary, secondary and tertiary deformation zones for an arbitrary cutting tool shape. Since there are still fundamental difficulties in modeling the behavior of metal during cutting, where the strain and strain rates reach to very high values, two dimensional cutting operations have been analyzed, but with tools having arbitrary cutting edge and rake face shapes. The slip line field diagram of a tool with chamfer edge is shown in Figure 3.

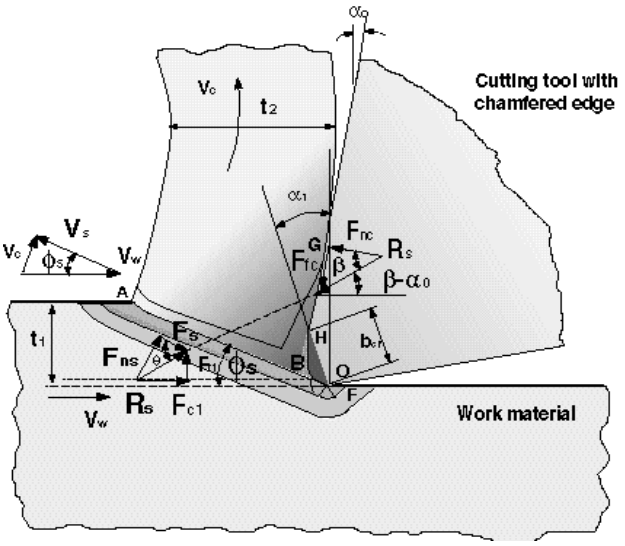

Figure 3: Slip line field model of chamfered tool.

Chamfered cutting edges are used on carbide and CBN tools for the high speed machining of hardened tool and die steels. The chamfer strengthens the wedge against chipping caused by thermal and mechanical stresses. The slip line field is modeled in such a way that the metal is trapped over the chamfer and incoming chip material flows over it. After the chip moves over the chamfer zone, it is approximated that the sticking and sliding friction zone lengths are equal. The total contact length on the rake face is predicted from force equilibrium [9]. The temperature modified flow stress of the material is identified from orthogonal cutting tests conducted with sharp tools [8]. The cutting forces and temperature contributed in the primary shear, chamfer, sticking and sliding zones are expressed as a function of unknown shear angle, and known friction constants on the rake face and temperature modified flow stress in each zone. The total energy consumed in all deformation zones are expressed mathematically, and minimum energy principal is used for the prediction of shear angle

[10],[11]. The expression is quite nonlinear, therefore an iterative solution was necessary. The method leads to the prediction of maximum temperature at the rake face as well as cutting forces contributed by the chamfer and flat rake face zones. P20 mold steel is used as an example work material. The carbide and CBN tools have binding materials which have typically diffusion limits of 1300 and 1600 Celsius, respectively. The analysis indicated that the most optimal chamfer angle is about -15 degrees, and the undesirable tool temperature is reached when the cutting speed is above 240m/min for carbide tools and 500 m/min for CBN tools. The cut thickness was 0.06 mm/rev in dry machining tests. The affect of temperature on the diffusion wear can be seen from SEM pictures of tested CBN tools shown in Figure 4.

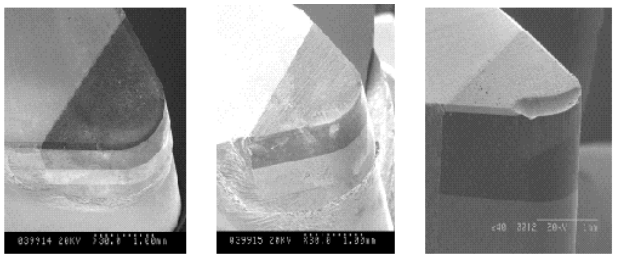

(a) cutting speed: V_w = 240 m/min (b) cutting speed: V_w = 400 m/min (c) cutting speed: V_w = 800 m/min

Figure 4: SEM pictures of chamfered CBN tools at different cutting speeds.

The slip line field analysis relies heavily on physical understanding and detailed modeling of cutting tool geometry, and only provides approximate solution in the average sense. A general approach, which can also provide more detailed information about the cutting zones, is through numerical modeling, and in particular, finite element modeling. In this approach, various tool geometry, cutting conditions and more sophisticated material and friction models can be incorporated, and the distribution of solution variables such as stress, strain and temperature may be obtained along with cutting forces. Nevertheless, owing to the large deformations and very high strain rates and temperatures involved in cutting process, such numerical modeling presents significant numerical and analytical challenges. An Arbitrary Lagrangian-Eulerian (ALE) formulation has been developed at UBC and applied for the prediction of cutting variables in machining [12],[13]. The developed ALE code can handle any two-dimensional tool geometry with rake face grooves, chamfers or edge radius on the cutting edge. Using this FE program, the machining of P20 mold steel by chamfered Carbide and CBN tools was analyzed and cutting variables such as temperature, strain, strain rate, stress distribution in the chip and residual stresses on the finish surface were predicted. The FE analysis of cutting with different chamfer angles and at different cutting speeds shows that there is indeed a trapped dead metal zone under the chamfer, but its size is dependent on tool geometry and cutting conditions. The dead zone diminishes as cutting speed increases, which may be attributed to material softening as a result of rapidly rising temperatures at high speed. Sample ALE results for cutting with chamfered tool are shown in Figure 5. Similar to slip line field analysis, FE also predicted maximum temperature of about 1200 Celsius on the rake face when the cutting speed and chip loads are 240m/min and 0.060mm/rev, respectively.

Slip line field analysis requires fundamental expertise, and FE requires significant amount of computation time. Both techniques can be best used by the trained engineers in metal cutting, and these techniques are useful for tool design. However, more practical methods are required for daily use in production floor for the selection of cutting speed and chip load which does not lead to thermal chipping or accelerated wear of the cutting edge. The author's group developed Finite Difference technique for both continuous machining and milling, which is integrated to our advanced cutting process simulation software used in industry. The finite difference technique uses average friction coefficient on the rake face, and considers sharp cutting edge. The temperature distribution in both chip and tool are predicted and displayed. When the temperature reaches to a critical threshold, which is about 1300 Celsius for carbide and about 1600 for CBN tools, the planner is warned for possible chipping or accelerated wear of the tool. The details of the finite difference modeling can be found in [14]. Briefly, in this temperature prediction model, the shear energy created in the primary zone, the friction energy produced at the rake face-chip contact zone and heat balance between the moving chip and tool are considered. Heat balance equations were determined in partial differential equations form for the chip and for the tool. The finite difference method was utilized for the solutions of the steady-state tool and chip temperature fields (Figure 6).

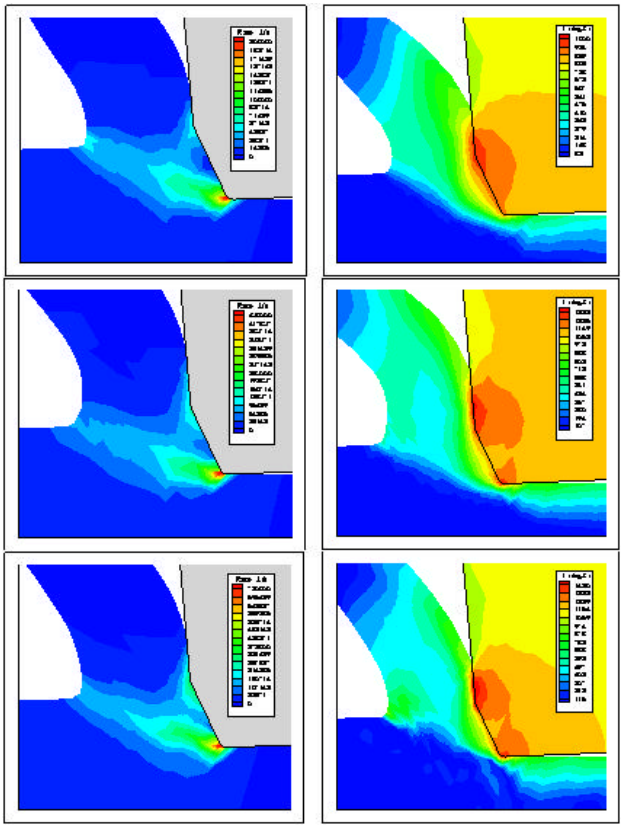

Figure 5: ALE analysis results for chamfered CBN tool.

In order to determine the transient temperature variation in the case of interrupted machining, the chip thickness was discretized along the time. Steady-state chip and tool temperature fields were determined for each of these discretized machining intervals. Based on thermal properties and boundary conditions, time constants were

determined for each discrete machining interval. By knowing the steady-state temperature and time constants of the discretized first order heat transfer system, an algorithm have been developed to determine the transient temperature variations in interrupted turning and milling operations (Figure 7).

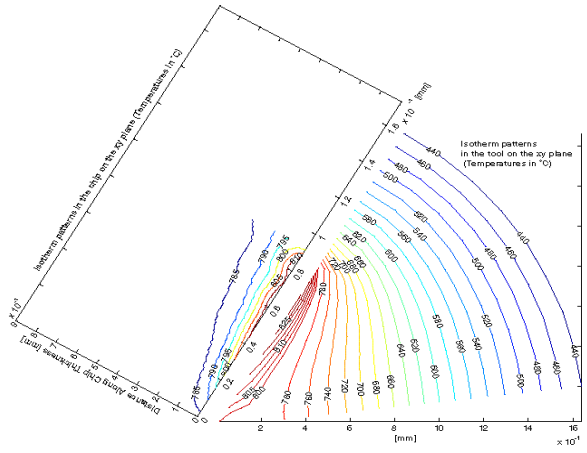

Figure 6: Predicted isotherm patterns of the chip during the machining of mild steel (cutting conditionas are given in [14] , temperatures in °C).

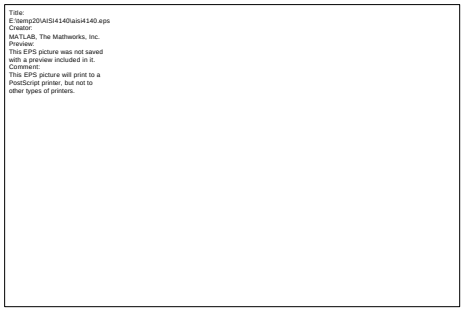

Figure 7: Measured and predicted average chip/tool interface temperature during milling AISI-4140 cutting conditions are given in [14].

It must be noted here that analysis methods in micro-mechanics of metal cutting heavily depend on not only the theory, but modeling of material behavior, such as friction field on the rake face and temperature-strain-strain rate dependent flow stress of the material in the deformation zones. If these physical parameters are not correctly identified, the methods used in the analysis of micro-mechanics of metal cutting may not yield reliable and practical results.

3 MECHANICS AND DYNAMICS OF MILLING

The author's group has spent considerable research effort in modeling the milling process in time and frequency domain. The time domain model is used to predict the cutting forces, torque, power, dimensional surface finish, and the amplitudes and frequency of vibrations during a milling operation. The frequency domain analysis leads to the identification of chatter vibration free spindle speeds, axial and radial depth of cut conditions in milling.

3.1 Time Domain Modeling of Milling

The work piece is fed linearly towards a rotating cutter having multiple teeth in milling operations. A point on the cutting edge of each tooth traces a trochoidal path [15], producing periodic chip loads at tooth passing frequency. The diagram of milling is shown in Figure 8.

If the radial width of cut is large, and the influence of structural vibrations is not considered in time domain, the cut thickness (*h*) can be approximated by assuming that the circular cutter body shifts at amount of feed per tooth at tooth passing periods,

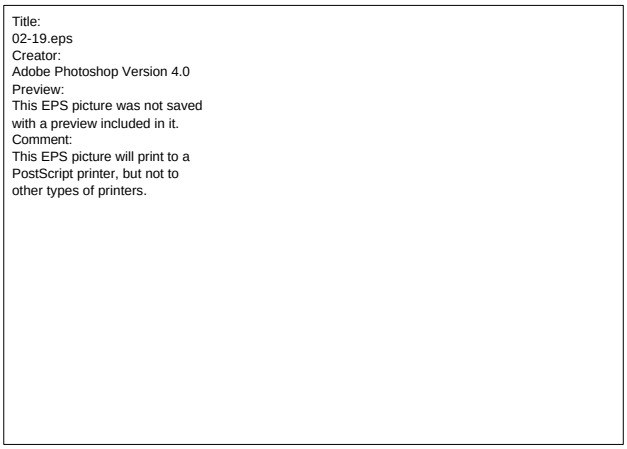

Figure 8: The geometry of milling process.

$$h(f) = c \sin f \qquad (9)$$

where ϕ is the angular immersion of the tooth measured from the axis normal to the feed and *c* is the feed per tooth [16]. However, if the analysis is expected to provide dimensional surface finish, feed marks and interaction with structural vibrations of the machine tool/fixture, true kinematics of dynamic milling are preferred. The author's group included the structural dynamic models of both work piece and cutter at the cutting edge - finish surface contact zones, see Figure 9. For example, a point on the cutting edge has coordinates, which are dependent on spindle speed, tool geometry, radial immersion and depth of cut:

$$P_t[x(t), y(t), z(t)] = f[R, W(t), x_t(t), y_t(t), z, t] \qquad (10)$$

where the cutter axis may vibrate away from the stationary spindle axis in feed ($x_t(t)$) and normal ($y_t(t)$) directions, and *z* is the elevation of cutting edge point from the tip of the cutter. The cutter has a radius of *R* and the spindle speed is $\Omega(t)$ which is used in calculating the angular immersion of the cutting edge, e.g. $\phi(t) = \Omega(t)t$. A point on the work piece surface moves linearly towards the rotating but vibrating cutter with a feed speed of *f*[*mm/s*], and its coordinates are dependent on the feed speed and part vibrations at that point:

$$P_w[x(t), y(t), z(t)] = f[x_w(t), y_w(t), z_w, f, t] \qquad (11)$$

where x_w, y_w are the amplitudes of work piece vibrations at this point, and *f* is the feed speed [mm/s]. The mathematical model of the kinematics, which is implemented in a computer algorithm needs quite a detailed presentation which can be found in [17],[18]. The intersection of $P_t(t)$ and $P_w(t)$ gives the cut surface.

The instantaneous chip thickness removed by $P_t(t)$ is most correctly evaluated by subtracting the present tool - work piece contact coordinates from the surface generated and tracked by $P_w(t)$ previously.

The subtraction is done along the radial vector which passes through the cutting edge point and vibrating cutter center, see Figure 9. The approach allows prediction of true chip load generated by the trochoidal motion of the milling tool and structural vibrations of both the cutter and work piece. The dimensional surface generation is rather automatic with this method, and the radial and axial run outs can be easily integrated to the model by defining each edge radius differently. Further details of the complete mathematical model of dynamic milling can be found in [19],[20],[21]. The structural vibrations of both the work piece and cutter are predicted by applying cutting forces to each structure at discrete time intervals [22],[23],[24],[25]:

$$\begin{aligned} m_x\ddot{x}(t) + c_x\dot{x}(t) + k_x x(t) &= F_x(t) \\ m_y\ddot{y}(t) + c_y\dot{y}(t) + k_y y(t) &= F_y(t) \end{aligned} \qquad (12)$$

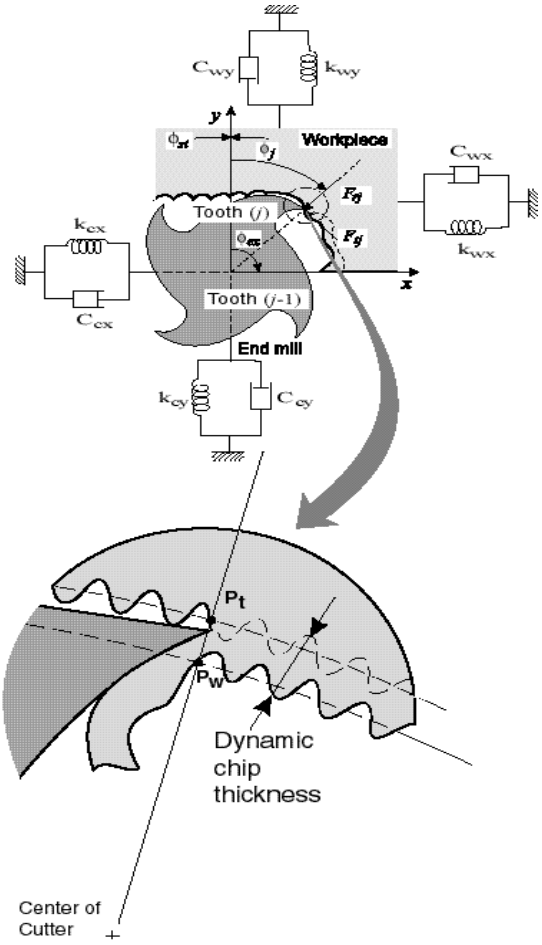

Figure 9: Surface and dynamic chip load evaluation using true kinematics of milling.

where *m*, *c*, *k* are the mass, damping and stiffness of either tool or work piece at the contact zone in the feed (*x*) or normal (*y*) directions. The differential cutting forces acting on a small cutting edge element with a height of *dz* in the tangential, radial and axial directions are expressed as :

$$\begin{aligned} dF_{t,j}(f,z) &= \left[K_{tc}h_j(f_j(z)) + K_{te}\right]dz \\ dF_{r,j}(f,z) &= \left[K_{rc}h_j(f_j(z)) + K_{re}\right]dz \\ dF_{a,j}(f,z) &= \left[K_{ac}h_j(f_j(z)) + K_{ae}\right]dz \end{aligned} \qquad (13)$$

where the cutting constants (K_{tc}, K_{rc}, K_{ac}) are either obtained from orthogonal to oblique cutting transformation as shown in Eq. (8) where the oblique angle is equal to helix angle in end mill and $K_{rc} = K_{fc}$, or using mechanistic approach as presented in the following. It must be noted that tooth number (*j*) at elevation *z* has different chip load than elsewhere if there is helix angle, run out or both. Proper geometric handling of the chip load calculation must be modeled as explained in [7]. The differential cutting forces can be projected in the three Cartesian axis as :

$$\begin{aligned} dF_{x,j}(f_j(z)) &= -dF_{t,j}\cos f_j(z) - dF_{r,j}\sin f_j(z) \\ dF_{y,j}(f_j(z)) &= +dF_{t,j}\sin f_j(z) - dF_{r,j}\cos f_j(z) \\ dF_{z,j}(f_j(z)) &= +dF_{a,j} \end{aligned} \qquad (14)$$

The differential cutting forces can be integrated digitally along the flute-work piece contact when the vibrations and true kinematics of milling are considered [26]. If only static forces are to be evaluated, the approximate chip load given in Eq. (9) is substituted in Eqs. (13) and (14), and integrated along the flute-work piece engagement length [27]:

$$\begin{aligned} F_{x,j}(f_j) = \Bigg\{ & \frac{c}{4k_b}\left[-K_{tc}\cos 2f_j(z) + K_{rc}\left[2f_j(z) - \sin 2f_j(z)\right]\right] \\ & + \frac{1}{k_b}\left[K_{te}\sin f_j(z) - K_{re}\cos f_j(z)\right]\Bigg\}_{z_j,1(f_j(z))}^{z_j,2(f_j(z))} \\ F_{y,j}(f_j) = \Bigg\{ & \frac{-c}{4k_b}\left[K_{tc}(2f_j - \sin 2f_j) + K_{rc}\cos 2f_j\right] \\ & + \frac{1}{k_b}\left[K_{te}\cos f_j(z) + K_{re}\sin f_j(z)\right]\Bigg\}_{z_j,1(f_j(z))}^{z_j,2(f_j(z))} \\ F_{z,j}(f_j) = \Bigg\{ & \frac{1}{k_b}\left[K_{ac}c\cos f_j(z) - K_{ae}f_j\right]\Bigg\}_{z_j,1(f_j(z))}^{z_j,2(f_j(z))} \end{aligned} \qquad (15)$$

where $z_{j,2}(\phi_j(z))$ and $z_{j,1}(\phi_j(z))$ are the upper and lower boundaries of helical flute engagement, helix lag parameter $k_\beta = 2\tan\beta / D$, and the instantaneous immersion angle of a flute *j* is $\phi_j(z) = \phi + j\phi_p - k_\beta z$ [7]. Here, ϕ is the angular position of reference tooth $j = 0$ at elevation *z* = 0, helix angle is β, cutter pitch angle $\phi_p = 2\pi / N$, the number of teeth is *N*, and the cutter has a diameter of *D*. If the helix angle is zero ($\beta = 0$), the differential element height is equal to the axial depth of cut (*dz* = *a*), and the instantaneous cutting forces are given by Eq.(15). Note that when the tooth is outside the entry (ϕ_{st}) and exit (ϕ_{ex}) angles of the cut, there is zero cutting force. The cutting forces contributed by all flutes are calculated and summed to obtain the total instantaneous forces on the cutter at immersion ϕ.

$$F_x(f)=\sum_{j=0}^{N-1}F_{x_j};\quad F_y(f)=\sum_{j=0}^{N-1}F_{y_j};\quad F_z(f)=\sum_{j=0}^{N-1}F_{z_j};\qquad (16)$$

Further details of computer algorithms in predicting the cutting forces are given in the text [7].

3.2 Mechanistic Modeling of Cutting Force Coefficients in Milling

When cutter has inserts with complex edge shape and non-uniform chip breaking grooves on the rake face, the orthogonal to oblique cutting transformation can not be used effectively. In this case, each insert must be calibrated mechanistically in order to identify its unique cutting force coefficient.

Mechanistic modeling approach has been quite popular in order to predict the cutting force coefficients quickly for a set of fixed cutter geometry and material couple. The cutting coefficient is either expressed as a constant number [28],[29],[30],[31], or as a function of cut thickness, cutting speed and tool geometry [32],[33],[34],[35],[36],[37]. Depending on the complexity of the tool geometry, behavior of the material at different chip loads and cutting speeds, there may be quite a number of machining tests to evaluate cutting coefficients mechanistically. The author adopted a simple cutting force relationship as shown in Eq. (13), which can be directly correlated with the unified orthogonal to oblique cutting mechanics transformation approach proposed by Armarego [38].

The average milling forces per tooth period is independent of helix angle, if the cutting coefficients are assumed to be chip load independent as expressed in Eq. (13). Integrating the cutting forces (Eq. (15)) in all three directions and dividing them by the pitch angle ($\phi_p = 2\pi/N$) gives the following average forces per tooth period :

$$\begin{aligned}
\overline{F}_x &= \left\{\begin{array}{l}\dfrac{Nac}{8p}\left[K_{tc}\cos 2f - K_{rc}\left[2f-\sin 2f\right]\right]\\ +\dfrac{Na}{2p}\left[-K_{te}\sin f + K_{re}\cos f\right]\end{array}\right\}_{f_{st}}^{f_{ex}}\\
\overline{F}_y &= \left\{\begin{array}{l}\dfrac{Nac}{8p}\left[K_{tc}\left[2f-\sin 2f\right]+K_{rc}\cos 2f\right]\\ -\dfrac{Na}{2p}\left[K_{te}\cos f + K_{re}\sin f\right]\end{array}\right\}_{f_{st}}^{f_{ex}}\\
\overline{F}_z &= \frac{Na}{2p}\left[-K_{ac}c\cos f + K_{ae}f\right]_{f_{st}}^{f_{ex}}
\end{aligned}\qquad (17)$$

Full immersion slot milling experiments are usually conducted at a range of feed rates (*c*), and average forces are measured during the cutting tests. The average cutting force measurements are plotted as a linear function of feed rate (*c*) as,

$$\overline{F}_{qe} = \overline{F}_{qc}c + \overline{F}_{qe}\qquad (q=x,y,z)\qquad (18)$$

where the intercepts at zero feed rate ($\overline{F}_{qe}$) correspond to edge forces [39]. By applying the boundary conditions of slot milling engagement ($\phi_{st}=0, \phi_{ex}=\pi$) to the average force equations (17), the average forces are found as:

$$\begin{aligned}
\overline{F}_x &= -\frac{Na}{4}K_{rc}c - \frac{Na}{p}K_{re}\\
\overline{F}_y &= +\frac{Na}{4}K_{tc}c + \frac{Na}{p}K_{te}\\
\overline{F}_z &= +\frac{Na}{p}K_{ac}c + \frac{Na}{2}K_{ae}
\end{aligned}\qquad (19)$$

From the measured values of Eq. (18) and equivalent expression Eq.(19), the cutting force coefficients are found mechanistically as:

$$\begin{aligned}
K_{tc} &= \frac{4\overline{F}_{yc}}{Na} \quad ; \quad K_{te} = \frac{p\overline{F}_{ye}}{Na}\\
K_{rc} &= \frac{-4\overline{F}_{xc}}{Na} \quad ; \quad K_{te} = \frac{-p\overline{F}_{xc}}{Na}\\
K_{ac} &= \frac{p\overline{F}_{zc}}{Na} \quad ; \quad K_{ae} = \frac{2\overline{F}_{ze}}{Na}
\end{aligned}\qquad (20)$$

It must be noted that the average forces in slotting may be close to zero due to force cancellation with certain number of teeth. In those cases, less than full immersion tests can be conducted by considering proper immersion boundaries in Eq. (17). The mechanistic cutting coefficients are usually quite accurate since they are calibrated directly from the milling tests conducted with the same cutter to be modeled. However, the mechanistic cutting coefficients are valid only for the particular cutter geometry tested, hence the method can not be used for cutter design purposes [40]. Some inserts may have varying rake angle along its rake face, hence the cutting coefficients may not be the same along the edge. In such cases, the cutting coefficients must be identified as a function of depth of cut or insert edge position. The resulting cutting force coefficient may be a polynomial function of insert location, which is presented in the following section.

3.3 Generalized Geometric Modeling of End Mills and Inserted Cutters

Variety of helical end mills and inserted cutters with varying geometry is used in industry. Helical cylindrical, helical ball, taper helical ball, bull nosed and special purpose end mills are widely used in aerospace, automotive and die machining industry. While the geometry of each cutter may be different, the mechanics and dynamics of the milling process at each cutting edge point are common. The author's group developed a generalized mathematical model of most helical end mills used in industry [41]. The end mill geometry is modeled by wrapping helical flutes around a parametric cutter envelope. The envelope of the cutter geometry is parametrically modeled using standard CAM definition, see Figure 10. The coordinates of a cutting edge point along the parametric helical flute are mathematically expressed.

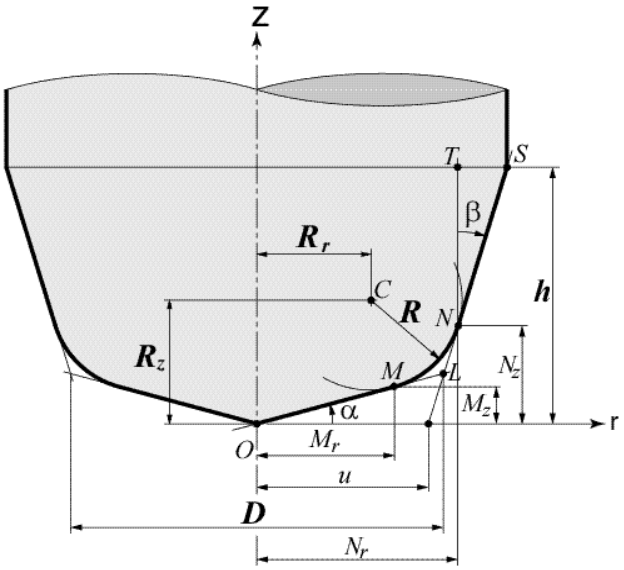

Figure 10: Parametric definition of general cutter geometry.

Sample end mills with helical flutes are shown in Figure 11. The chip thickness at each cutting point is evaluated by using the true kinematics of milling including the structural vibrations of both cutter and work piece, as explained in section 3.1. By digitally integrating the process along each cutting edge, which is in contact with the work piece, the cutting forces, vibrations, dimensional surface finish and chatter stability lobes for an arbitrary end mill can be predicted [18]. Experimental and simulation results are shown for sample end mills with complex geometry in the experimental section 5.

Inserted cutters are also modeled using a similar philosophy [41]. The insert geometry and distribution of inserts on the cutter body vary significantly in industry depending on the application. A generalized mathematical model of inserted cutters is developed. The edge geometry is defined in the local coordinate system of each insert, and placed and oriented on the cutter body using cutter's global coordinate system, see Figure 12. The cutting edge locations are defined mathematically, and used in predicting the cut thickness distribution along the cutting zone. Each insert may have a different geometry, such as rectangular, convex triangular or a mathematically definable edge. Each insert can be placed on the cutter body mathematically by providing the coordinates of insert center with respect to the cutter body center. The inserts can be oriented by rotating them around the cutter body, thus each insert may be assigned to have different lead and axial rake angles. By solving the mechanics and dynamics of cutting at each edge point, and integrating them over the edge contact zone, it is shown that the milling process can be predicted for any inserted cutter. As noted earlier, the cutting coefficients may be different for each insert, and may even vary along the insert's cutting edge, which are considered in the mathematical model. A sample application of inserted cutter modeling and analysis is provided in the experimental section 5.

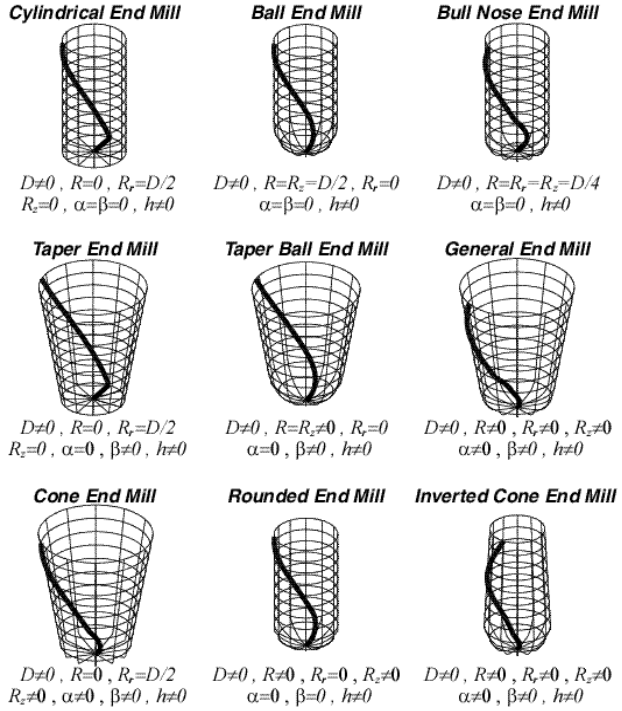

Figure 11: Helical cutting edges wrapped around end mills.

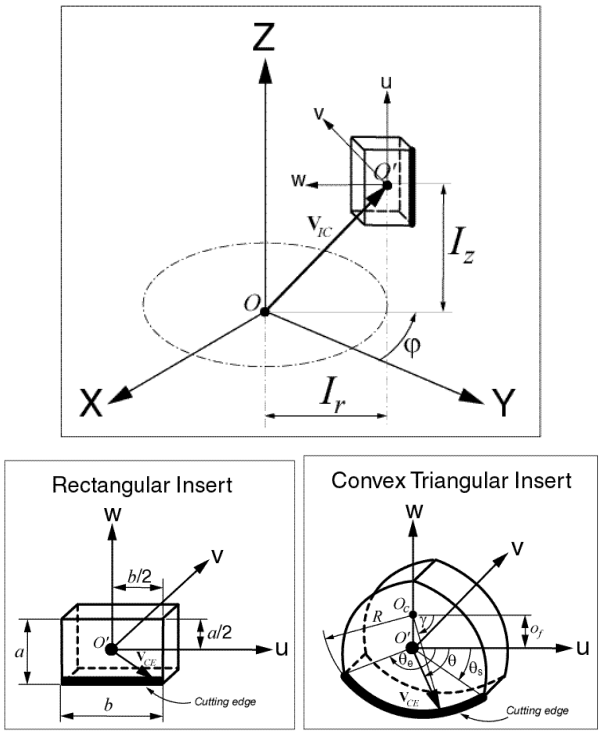

Figure 12: Geometric modeling of inserted cutters.

4 CHATTER STABILITY IN MILLING

Chatter vibrations are still most limiting factor in preventing high material removal rates in machining. Unfortunately, chatter is avoided by reducing spindle speed and depth of cut, hence the productivity, in most production floors. Since Tlusty [42] and Tobias [43], there has been significant amount of research and understanding accomplished in chatter. However, due to the complexity of chatter, its physics and mathematics, the machine tool and manufacturing engineers somehow have not absorbed the knowledge. The author's group

has spent considerable effort and years in modeling and understanding the chatter vibrations, and has been successful in using and transferring the methods to industry which led to noted productivity gains.

Chatter occurs due to relative structural vibrations between the tool and the work at the cutting zone. Consider a simple case where the cutter has structural flexibility in the feed (*x*) and normal (*y*) directions, see Figure 9. When a tooth enters the cut, it excites the natural modes of the structure, hence leaving a wavy surface finish behind due to transient vibrations. When the second tooth comes, it also experiences vibrations and leaves a wavy surface behind. The true dynamic chip thickness is therefore dependent on not only the rigid body motion (i.e. feed and spindle speed) but on the present and past vibration marks left on the cut surface as well. If the present (i.e. inner wave) and previous (i.e. outer wave) are parallel or *in phase*, the dynamic chip load would still remain the same regardless of vibrations. However, when the phase shift is close to *180* degrees, than the chip thickness oscillates between two extreme values. If the system can not absorb the energy, the process becomes unstable, and the vibrations may grow exponentially until the tool jumps out of cut or breaks. Since the cutting forces are proportional to the chip thickness, they too oscillate with large magnitudes, which may damage the cutter, work piece or spindle bearings. Chatter occurs close to one of the dominant modes of the machine tool structure. At slow speeds and heavy cuts, the chatter is mainly dominated by the low frequency spindle and machine tool column-table modes. Higher natural modes of the machine tool structure such as spindle, or slender end mill may dominate the chatter at higher speeds.

Budak and Altintas [44] developed a chatter theory specifically for milling operations. The details of the derivations can be found in the text [7] and articles [45], [46],[47] published by the author's group. The solution is briefly summarized here. The chatter stability equation is reduced to the following quadratic form:

$$\begin{aligned} &a_0\Lambda^2 + a_1\Lambda + 1 = 0 \\ &a_0 = G_{xx}(iw_c)G_{yy}(iw_c)(a_{xx}a_{yy} - a_{xy}a_{yx}) \\ &a_1 = a_{xx}G_{xx}(iw_c) + a_{yy}G_{yy}(iw_c) \end{aligned} \tag{21}$$

and G_{xx}, G_{yy} are the direct frequency response functions of the machine tool/work piece structure measured at the cutter tip, and Λ is the eigenvalue. The cross frequency response functions can also be included as shown in [45]. The directional factors are dependent on the cutter engagement angles with the work piece, and given as :

$$\begin{aligned} a_{xx} &= 0.5\left[\cos 2f - 2K_r f + K_r \sin 2f\right]_{f_{st}}^{f_{ex}} \\ a_{xy} &= 0.5\left[-\sin 2f - 2f + K_r \cos 2f\right]_{f_{st}}^{f_{ex}} \\ a_{yx} &= 0.5\left[-\sin 2f + 2f + K_r \cos 2f\right]_{f_{st}}^{f_{ex}} \\ a_{yy} &= 0.5\left[-\cos 2f - 2K_r f - K_r \sin 2f\right]_{f_{st}}^{f_{ex}} \end{aligned} \tag{22}$$

where $K_r = K_{rc} / K_{tc}$. The eigenvalue Λ is obtained as:

$$L = -\frac{1}{2a_0}(a_1 \pm \sqrt{a_1^2 - 4a_0}) = L_R + iL_I \tag{23}$$

The critical depth of cut for chatter stability limit is given by,

$$a_{\lim} = -\frac{2pL_R}{NK_t}(1 + k^2) \tag{24}$$

where $\kappa = \Lambda_I / \Lambda_R$ and smaller axial depth of cut is accepted from the two values of the eigenvalues used. The corresponding tooth period ($T[s]$) and spindle speed $(n[rev/\min])$ are given by,

$$T = \frac{1}{w_c}(e + 2kp) \quad \rightarrow \quad n = \frac{60}{NT} \tag{25}$$

where the phase shift between the inner and outer chip surface waves is $\varepsilon = 3\pi - 2\tan^{-1}\kappa$, and *k* = 0, 1, 2, 3, … represents the number of lobes or the number of waves left on the cut surface within one tooth period. When the axial depth of cut and spindle speed is selected under the chatter stability limits defined by the depth of cut and spindle speed values predicted by the theory, the chatter vibrations are avoided and higher material removal rates can be obtained. The theory presented here is based on linear stability laws, which do not consider time varying cutting coefficients, tool jumping out of cut, and process damping caused by the friction of tool flank with the wavy finish surface . However, a time domain simulation of chatter stability, which is also developed by the author's group as explained in the previous section, considers all of the non-linearities, and is used to predict forces, vibrations, torque, power and surface form errors. The author's group compared their the time domain and frequency domain solutions, as well as experimental observations, at a variety of cutting conditions with structural dynamic modes. The agreement was found to be very satisfactory as supported by the experimental results presented in the following section.

5 INDUSTRIAL APPLICATION AND EXPERIMENTAL RESULTS

The milling algorithms presented in the article have been applied in modeling some sophisticated end mills and inserted cutters for the benefit of industrial partners of our laboratory. Some of the applications are presented here.

Tapered helical ball end mills are used in five-axis peripheral milling of jet engine compressors made of Titanium alloy Ti6Al4V. The orthogonal cutting parameters of Ti6Al4V are modeled from tube turning tests and given in Table 1.

The cutter geometry, and predicted and measured cutting forces are shown in Figure 13.

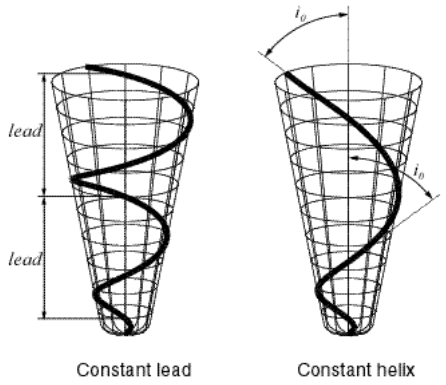

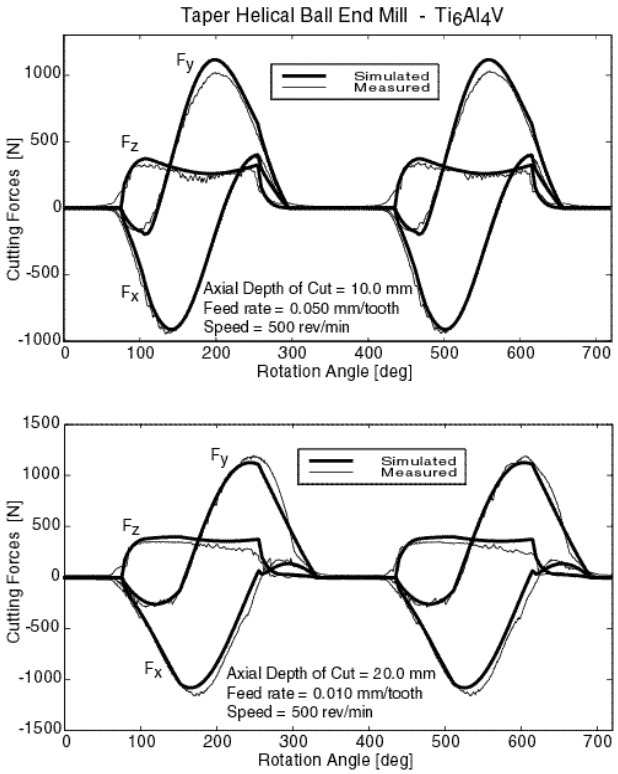

Figure 13: Predicted and measured cutting forces for a tapered helical ball end mill.

Table 1:Orthogonal cutting parameters of Ti6Al4V.

$t_s = 613(MPa)$
$b_a = 19.1 + 0.29a_r (\deg)$
$r_c = C_0 h^{c_1}$
$C_0 = 1.755 - 0.028a_r$
$C_1 = 0.331 - 0.0082a_r$
$K_{te} = 24(N/mm)$
$K_{fe} = 43(N/mm)$

The tapered cutter has a constant lead, therefore it has a varying helix or oblique angle along the helical flute [41]. The cutting coefficients vary at each point along the cutting edge, and they are modeled by orthogonal to oblique cutting transformation as proposed by Armarego [6]. Similarly, a cutter with two coated circular inserts is used in milling Ti6Al4V. The geometric model, picture of the cutter, and the predicted and measured milling forces are presented in Figure 14.

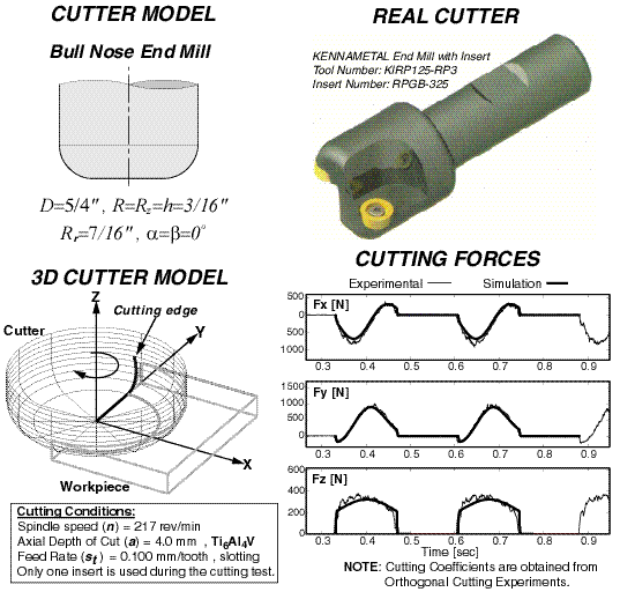

Figure 14: Predicted and measured cutting forces for a cutter with circular inserts.

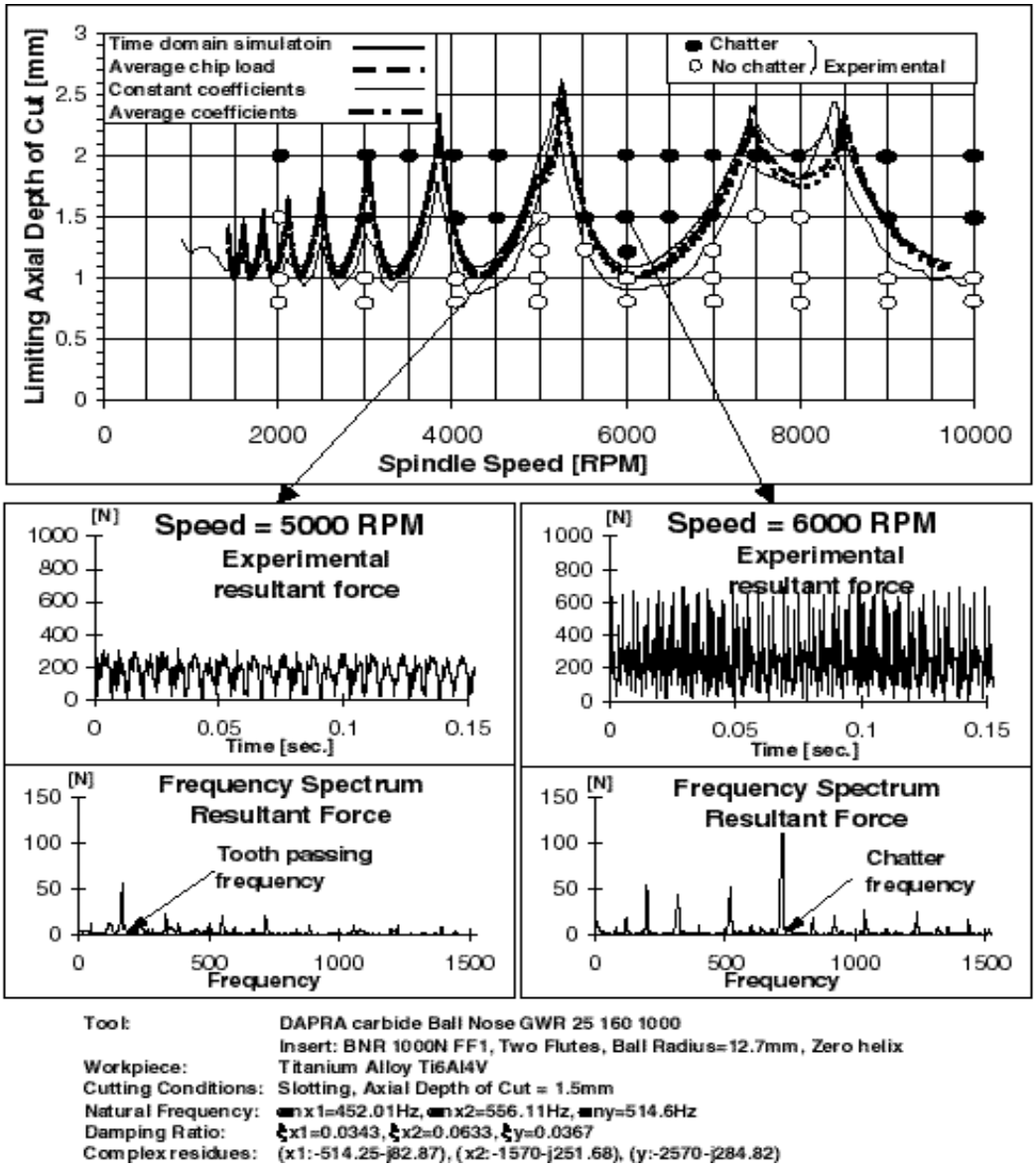

Tool:	DAPRA carbide Ball Nose GWR 25 160 1000
	Insert: BNR 1000N FF1, Two Flutes, Ball Radius=12.7mm, Zero helix
Workpiece:	Titanium Alloy Ti6Al4V
Cutting Conditions:	Slotting, Axial Depth of Cut = 1.5mm
Natural Frequency:	ω_{x1}=452.01Hz, ω_{x2}=556.11Hz, ω_{y}=514.6Hz
Damping Ratio:	ζ_{x1}=0.0343, ζ_{x2}=0.0633, ζ_{y}=0.0367
Complex residues:	(x1:-514.25-j82.87), (x2:-1570-j251.68), (y:-2570-j284.82)

Figure 15: Predicted and experimentally observed chatter stability lobes, frequency spectrum and dimensional surface finish in ball end milling of Titanium Ti6Al4V.

Again, the orthogonal cutting parameters presented in Table 1 is used in oblique transformation [48],[49]. The method is applied in predicting chatter stability lobes, as well as the forces, dimensional surface finish, vibration amplitudes when chatter is present during milling. Note that average, constant cutting coefficients are used in predicting the chatter stability solved in the frequency domain. The chatter stability is also predicted in time domain, where the varying cutting coefficients and non-linearities in the process are considered [20], [21]. A sample ball end milling of Ti6Al4V is presented in Figure 15. The details of the machine dynamics and cutter geometry can be found in [26],[46]. As indicated before, the analytical frequency domain chatter stability solution agrees well with the time domain simulation. An accurate time domain solution takes number of hours, whereas the frequency domain solution takes few seconds with an acceptable accuracy. However, both time domain and frequency domain solutions may lead to inaccurate predictions due to neglected process damping, which can be identified only experimentally for a reliable solution.

The stability lobes allow the process planner to select the highest possible depth of cut and spindle speed, i.e. material removal rate, without causing chatter vibrations. Because the author's group uses true kinematics of milling with the presence of vibrations, the dimensional surface errors, vibration amplitudes and frequency, and the cutting forces are predicted with a very reasonable accuracy. By considering variety of end mill geometry, about 85% of the force predictions have less than 10% deviation from measurements, with a maximum deviation in all cases less than 20% [21][54]. It can be stated that the orthogonal to oblique transformation is quite useful in predicting the performance of the end mills during the design stage before they are manufactured. However, for an accurate prediction, the cutting edges must not have chip breakers or chamfers, and orthogonal cutting parameters must be carefully identified from orthogonal tube turning tests.

A sample multi-level inserted milling cutter and its geometric model is shown in Figure 16. There are two flutes and four rectangular inserts on each flute. One series of inserts have 10 degrees of helix, while the second series have 20 degrees helix. The cutting coefficients of each insert type are modeled mechanistically, and given in Table 2 for inserts with 10 degrees helix angle [50].

Table 2: Mechanistically modeled cutting coefficients for inserts shown in Figure 16. (z is the insert edge length.)

	Cutting Coef.	Fitted curve
10° helix angle	K_{tc} [N/mm^2]	$7.9z^2 - 90.4z + 1073.5$
	K_{rc} [N/mm^2]	$25.98z^2 - 222.3z + 795.1$
	K_{ac} [N/mm^2]	$19.55z^2 - 159.4z + 294.55$
	K_{te} [N/mm]	$-0.34z^2 - 1.91z + 38.78$
	K_{re} [N/mm]	$-3.15z^2 + 22.98z + 23.80$
	K_{ae} [N/mm]	$-2.66z^2 + 27.56z - 54.80$
20° helix angle	K_{tc} [N/mm^2]	$-5.6z^2 + 22.76z + 925.4$
	K_{rc} [N/mm^2]	$-13.0z^2 + 85.6z + 409.1$
	K_{ac} [N/mm^2]	$-15.3z^2 + 181.9z - 227.6$
	K_{te} [N/mm]	$-0.04z^2 - 2.04z + 33.86$
	K_{re} [N/mm]	$-0.46z^2 + 1.38z + 53.86$
	K_{ae} [N/mm]	$-0.25z^2 + 2.56z - 6.92$

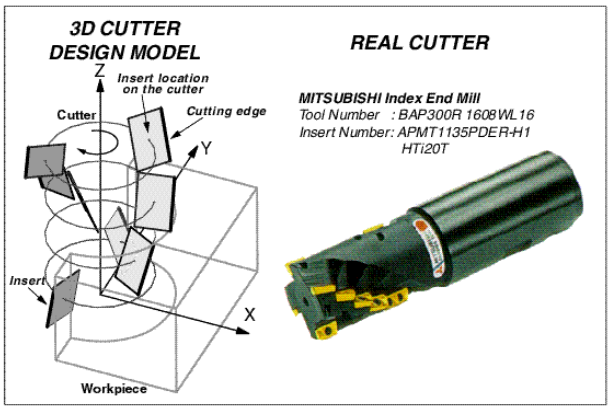

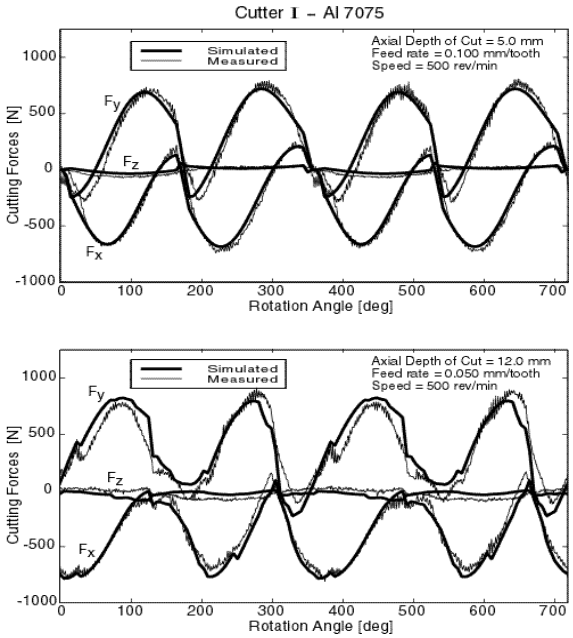

Figure 16: Predicted and experimentally evaluated cutting forces produced by a two fluted four layer indexed cutter.

Sample comparison of predicted and measured cutting forces are shown in Figure 16. The chatter stability lobes were predicted in time domain using the cutting coefficients given in Table 2. By using average cutting coefficients along the insert edge length (*z*) the stability lobes are predicted in the frequency domain as well, see Figure 17. The model considers the tool geometry, feed and speed, as well as vibrations, which are used in predicting the cutting forces and dimensional surface finish, described by the kinematics of milling and vibrations. It can be seen that the simulated and experimentally obtained stability lobes chatter frequency and dimensional surface finish are in good agreement.

The author's group developed various methods in improving milling process planning and productivity. The milling process is integrated to solid model based CAD system, and part geometry dependent milling process is simulated and the feed at each NC block is optimized [16],[27]. Radial width of cut and feed are analytically identified to lead minimum static form errors when thin webs are milled with long slender end mills [51], [52],[53],[54]. The influence of variable pitch cutters on dimensional surface finish is analyzed, and the pitch angle of the cutter is tuned to dominant structural mode in the frequency domain which allows chatter free milling at a desired speed and depth of cut [47],[55]. The knowledge of milling process modeling is applied to monitoring and adaptive control of milling operations, spindle design as well as high speed feed drive control system which are not listed here.

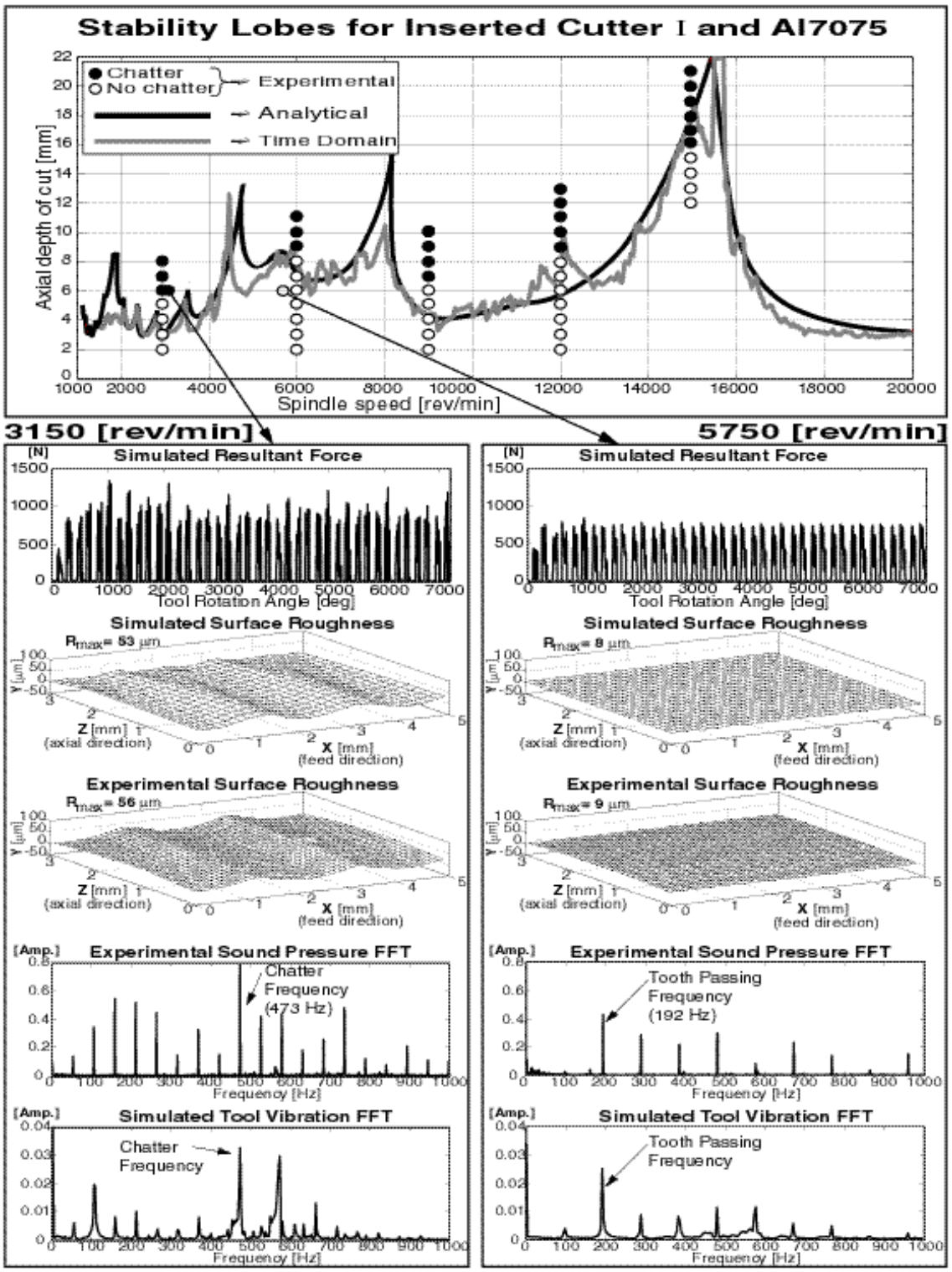

Figure 17: Stability lobes for Al-7075 with cutter shown in Figure 16. Cutting Conditions: Half immersion down milling with 0.05mm/tooth feed rate.

6 CONCLUDING REMARKS

A brief overview of the research conducted by the author's research group is presented here. The detailed analysis of metal cutting is attempted using slip line field and Finite Element modeling techniques, which are called micro-metal cutting mechanics here. Micro-metal cutting mechanics include the behavior of the plastically deformed metal in the cutting, rake face-chip interface and flank -finish work piece interface zones. The success of the analysis models is heavily dependent on the ability to model the material behavior during cutting, tool rake face - chip friction contact, and interaction between the flank and elasto-plastically deformed finish surface. We have not been able to sufficiently understand and model this phenomenon up to the present. The material models are best estimated from orthogonal cutting tests due to presence of high strains, strain rates and temperature distribution in metal cutting zone. However, since we are not able to measure the strain, strain rate and

temperature distribution in the chip and shear zone accurately, the predicted flow stresses are still very approximate. The same criticism is valid for chip-rake face interface, where the friction field may vary significantly depending on the state of material. Instruments and methods, which allow accurate measurement of temperature and tool-chip interface pressure, have yet to be developed for deeper understanding and modeling of micro-mechanics of metal cutting.

The same argument is not valid for macro mechanics models, which are heavily dependent on experimentally identified average values of pressure and temperature in the cutting zone. It is possible to predict the cutting forces, torque, power, and dimensional surface finish and chatter stability with satisfactory accuracy using the present knowledge of the macro-mechanics of milling operations. We are still not able to analytically model the interaction between the flank face of the tool and wavy finish surface, i.e. process damping, in machining which may suppress the chatter vibrations at the expense of accelerated tool wear. However, this problem also belongs to the micro-mechanics of metal cutting research.

ACKNOWLEDGEMENTS

The research reviewed in this article is based on the thesis of graduate students supervised by the author. The work of following graduate students and visiting academics have been most relevant to the article. A. Spence (Ph.D., 1992), E. Budak (Ph.D., 1995), S. Engin (Ph.D., 1999), M. Movahheddy (Ph.D.2000), Dr. G. Yucesan (1992), Dr. K. Sirashe (1995), Dr. E. Shamoto (1996), Dr. I. Lazoglu (1999-2000), D. Montgomery (M.A.Sc. 1990), P. Lee (M.A.Sc. 1996), H. Ren (M.A.Sc., 1998), M.L. Campomanes (M.A.Sc. 1998). The author's research laboratory received financial and material support from various research centers and companies. The major funding sources include Natural Sciences and Engineering Council of Canada (NSERC), Pratt & Whitney Canada, General Motors USA and Canada, Boeing Corporation, Mitsubishi Materials, Weiss, Milacron and Mori Seiki.

REFERENCES

[1] van Luttervelt, K., Childs, T.H.C., Jawahir, I.S., Klocke, F., Venuvinod, P.K., 1998, "Present Situation and Future Trends in Modeling of Machining Operations", Annals of CIRP, vol.47/2, pp. 587-626.

[2] Ehmann, K. F., Kapoor, S. G., DeVor, R.E., and Lazoglu, I., 1997, “Machining Process Modeling: A Review”, Journal of Manufacturing Science and Engineering Transaction of the ASME, Vol. 119(No.4-B), pp.655-663.

[3] Tlusty, J., 1999, 'Manufacturing Processes and Equipment”, Prentice Hall, Inc.

[4] Kienzle, O., Victor, H., 1957, “Spezifische Schnittkrafte bei der Metallbearbeiting”, Werkstofftechnik und Maschinenbau, 47/5, pp.224-225.

[5] Metcut Research Associates Inc., Cincinnati, OH. 1972, “Machining Data Handbook”, 2nd Edition.

[6] Armarego, E., Brown,J., 1969, " The Machining of Metals", Prentice Hall, Inc.

[7] Altintas,Y., 2000, "Manufacturing Automation: Metal Cutting Mechanics, Machine Tool Vibrations, and CNC Design", Cambridge University Press.

[8] P.L.B. Oxley, 1989, *Mechanics of Machining-an analytical approach to assessing machinability*, Ellis Horwood Limited.

[9] Ren, H., Altintas, Y., "Mechanics of Machining with Chamfered Tools", Trans. ASME, Manufacturing and Engineering and Science (in press, October 2000).

[10] Merchant, M.E., 1945, ``Mechanics of the Metal Cutting Process, II. Plasticity Conditions in Orthogonal Cutting ", *J. Appl. Phys.*, Vol.16, pp.318-324.

[11] Shamoto, E., Altintas, Y., 1999, "Prediction of Shear Angle in Oblique Cutting", Transactions of ASME Journal of Engineering for Manufacturing Science and Engineering, vol. 121, pp. 399-407.

[12] Movahhedy, M. S. Gadala and Y. Altintas, 2000, "Simulation of Chip Formation in Orthogonal Metal Cutting Process: An ALE Finite Element Approach", Machining Science and Technology, vol.4,pp.15-42.

[13] Movahhedy, M.R., 2000, "ALE Simulation of chip formation in orthogonal metal cutting process ", Ph.D. Thesis, Department of Mechanical Engineering, The University of British Columbia, Vancouver, B.C., Canada.

[14] Lazoglu I, Altintas Y, “Temperature prediction for Continuous machining and Milling Processes.” Trans ASME J Manufacturing Science and Engineering (October 1999)

[15] Martelotti,M.E.,1999, "An Analysis of the Milling Process", Transactions of ASME, vol.63,pp.677-700.

[16] Altintas, Y., Spence, A., 1991, "End Milling Force Algorithms for CAD Systems", Annals of CIRP, Vol. 40/1, pp. 31-34.

[17] Montgomery, D., Altintas, Y.,1991, "Mechanism of Cutting Force and Surface Generation in Dynamic Milling", Transactions of ASME, Journal of Engineering for Industry, Vol. 113, pp. 160-168.

[18] Altintas, Y., Lee, P., "A General Mechanics and Dynamics Model for Helical End Mills", Annals of CIRP, Vol. 45/1, pp. 59-64, 1996.

[19] Montgomery,D. ,1990, " Milling of Flexible Structures", M.A.Sc. Thesis, Department of Mechanical Engineering, The University of British Columbia, Vancouver, B.C., Canada.

[20] M. Campomanes, 1998, "Dynamic of Milling Flexible Structure ", M.A.Sc. Thesis, Department of Mechanical Engineering, The University of British Columbia, Vancouver, B.C., Canada.

[21] Lee, P.W., 1996, "Mechanics and Dynamics of ballend Milling ", M.A.Sc . Thesis, Department of Mechanical Engineering, The University of British Columbia, Vancouver, B.C., Canada.

[22] Tlusty, J., and Ismail, F., 1981, “Basic Nonlinearity in Machining Chatter, “Annals of the CIRP, Vol. 30/1, pp. 299-304.

[23] Smith, S., and Tlusty, J., 1993, “Efficient Simulation Programs for Chatter in Milling” Annalsof the CIRP, Vol. 30, pp. 21-25.

[24] Shin, Y. C., and Waters, A. J., 1994, “ Face Milling Process modeling with Structural Nonlinearity,” Transactions of NAMRI/SME, Vol. 22, pp. 157-164.

[25] Elbestawi, M.A., Ismail, F., Du, R., and Ullagaddi, B.C., 1994,“ Modeling Machining Dynamics Including Damping in the Tool-Workpiece Interface, “ ASME journal of Engineering for Industry, Vol. 116, pp. 435-439.

[26] Altintas, Y., Lee, P.,1998, "Mechanics and Dynamics

of Ball End Milling Transactions of ASME, Journal Manufacturing Science and Engineering,vol.120, pp.684-692.

[27] Spence, A., Altintas, Y., 1994, "A Solid Modeller Based Milling Process Simulation and Planning System", Transactions of ASME Journal of Engineering for Industry, Vol. 116, pp. 61-69.

[28] Sabberwal, A.J.P., 1961, "Chip Section and Cutting Force during the Milling Operation", Annals of CIRP, vol.10,pp.197-203.

[29] Tlusty, J., MacNeil, P.,1975, "Dynamics of Cutting Forces in End Milling" Annals of the CIRP, vol.24,pp.21-25.

[30] Gygax, P.E.,1979, "Dynamics of Single Tooth Milling", Annals of the CIRP, Vol. 28/1,pp.65-70.

[31] Yellowley, I.,1985, "Observations of the Mean Values of Forces, Torque and Specific Power in the Peripheral Milling Process", Int. J. mach. Tool Des. Res. Vol. 25, No. 4.

[32] Fu, H.J., Devor, R.E., Kapoor, S.G.,1984, "A Mechanistic Model for the Prediction of the Force System in Face Milling Operations", ASME J. of Eng. for Ind., Vol. 106.pp.81-88.

[33] DeVor, R.E., Kline, W.A., and Zdeblick, W.J., 1980, "A Mechanistic Model for the Force System in End Milling with Application to Machining Airframe Structures," 8th NAMRC Proc., pp. 297-303.

[34] Kline, W.A., DeVor, R.E., 1983, "The Effects of Runout on Cutting Geometry and Forces in End Milling", Int. J. of Mac. Tool. Des. Res., Vol. 23, No, 2/3, pp. 123-140.

[35] Ber, A., Rotberg, J., Zombach, S., 1988, "A Method for Cutting Force Evaluation of End-Mill", CIRP Annals, vol. 37/1, pp. 37-40.

[36] Endres, W.J., DeVor, R.E., and Kapoor, S.G., 1995,"A Dual Mechanism Approach to the prediction of Machining Forces, Part1: Model Development," ASME Journal of Engineering for Industry, Vol. 117, pp.536-533.

[37] Lazoglu, I., Liang, S. Y., 2000,"Modeling of Ball-End Milling Forces With Cutter Axis Inclination", Journal of Manufacturing Science and Engineering Transaction of the ASME, Vol. 122(No.1), pp.3-11.

[38] Armarego, E.J.A., 1994, "Material Removal Processes – An Intermediate Course", Department of Mechanical Engineering, The University of Melbourne.

[39] Budak, E., Altintas, Y., Armarego, E. J. A.,1996, "Prediction of Milling Force Coefficients from Orthogonal Cutting Data", Transactions of ASME, Journal of Manufacturing Science and Engineering (former name: Journal Engineering for Industry), Vol. 118/2, pp. 216-224.

[40] Yucesan, G., Altintas, Y.,1994, "Improved Modeling of Cutting Force Coefficients in Peripheral Milling", International Journal of Machine Tools \& Manufacture, Vol. 34/4, pp. 473-487.

[41] Engin, S., Altintas, Y., "Generalized Modeling of Milling Mechanics and Dynamics: Part I- End Mills, Part II- Inserted Cutters", IMECE ASME Winter Annual Meeting, Nashville, Nov. 1999.

[42] Koenigsberger, F. and Tlusty, J., 1967, *Machine Tool Structures-Vol.1: Stability Against Chatter*, Pergamon Press.

[43] Tobias, S.A, 1965. *Machine Tool Vibration*. Blackie and Sons Ltd.

[44] Altintas, Y., Budak, E., 1995,"Analytical Prediction of Stability Lobes in Milling", Annals of CIRP, Vol. 44/1, pp. 357-362.

[45] Budak, E., Altintas, Y., 1998, "Analytical Prediction of Chatter Stability Conditions for Multi-Degree of Systems in Milling. Part I: Modeling, Part II: Applications", Transactions of ASME, Journal of Dynamic Systems, Measurement and Control, vol.120, pp.22-36.

[46] Altintas, Y., Shamoto, E., Lee, P., Budak, E., 1999, "Analytical Prediction of Stability Lobes in Ball End Milling", Transactions of ASME Journal of Manufacturing Science and Engineering, vol.121, pp.586-592.

[47] Altintas,Y., Engin, S., Budak, E., 1999, " Analytical Prediction of Chatter Stability and Design for Variable Pitch Cutters", Trans. ASME, Manufacturing and Engineering and Science, vol.121, pp.173-178.

[48] Yucesan, G., Altintas, Y., 1996,"Prediction of Ball End Milling Forces", Transactions of ASME, Journal Engineering for Industry, vol. 118/1, pp.95-103.

[49] Lee, P., Altintas, Y., 1996, "Prediction of Ball End Milling Forces from Orthogonal Cutting Data", International Journal of Machine Tools and Manufacture, Vol. 36/9, pp.1059-1072.

[50] Engin, S., '1999, 'Mechanics and Dynamics of Milling with Generalized Geometry ", Ph.D. Thesis (MAL-UBC), Faculty of Mechanical Engineering, Istanbul Technical University, Gumussuyu, Istanbul, Turkey.

[51] Altintas, Y., Montgomery, D., Budak, E., 1992, "Dynamic Peripheral Plate Milling of Flexible Structures", Transactions of ASME, Journal of Engineering for Industry, Vol. 114, pp. 137-145.

[52] Budak, E., Altintas, Y., 1994, "Peripheral Milling Conditions for Improved Dimensional Accuracy", International Journal of Machine Tools \& Manufacture, Vol. 34/7, pp. 907-918, 1994.

[53] Budak, E., Altintas, Y., 1995, "Modelling and Avoidance of Static Form Errors in Peripheral Milling of Plates", Int. J. Mach. Tools \& Manufacture, Vol. 35/3, pp. 459-476.

[54] Budak, E., 1995, "Mechanics and dynamics of Milling Thin Walled Structures ", Ph.D. Thesis, Department of Mechanical Engineering, The University of British Columbia, Vancouver, B.C., Canada.

[55] Shirashe, K., Altintas, Y., 1996, "Force and Surface Generation Mechanism with Variable Pitch Helical End Mills", International Journal of Machine Tools and Manufacture, Vol. 36/5, pp.567-584.